


 CrossMark  
 click for updates

Cite this: RSC Adv., 2015, 5, 21897

## Raman spectroscopic studies and DFT calculations on $\text{NaCH}_3\text{CO}_2$ and $\text{NaCD}_3\text{CO}_2$ solutions in water and heavy water†

 Wolfram W. Rudolph<sup>\*a</sup> and Gert Irmer<sup>b</sup>

Sodium acetate and sodium acetate-d<sub>3</sub> solutions in water and heavy water were studied using Raman spectroscopy over a wide concentration range and from low wavenumbers (40  $\text{cm}^{-1}$ ) up to 4200  $\text{cm}^{-1}$ . In the terahertz region the broad breathing mode Na–O at 189  $\text{cm}^{-1}$  was detected as well as a broad shoulder at 245  $\text{cm}^{-1}$  of the restricted translation band of acetate–water. Fundamental modes of  $\text{CH}_3\text{CO}_2^-(\text{aq})$  and acetate-d<sub>3</sub>,  $\text{CD}_3\text{CO}_2^-(\text{aq})$ , were assigned and discussed according to pseudo  $C_s$  symmetry. The vibrational isotope effect of the  $\text{CH}_3/\text{CD}_3$  group was observed and the Teller-Redlich product rule confirmed the assignments. Additionally, band assignments of  $\text{CH}_3\text{CO}_2^-$  and  $\text{CD}_3\text{CO}_2^-$  in heavy water were reported and discussed. By changing from  $\text{H}_2\text{O}$  to  $\text{D}_2\text{O}$ , relatively strong H-bonding between the oxygen atoms of acetate causes a change in the vibrational energy levels of the dissolved acetate. The symmetric stretching mode of the  $\text{CO}_2$  group for  $\text{CH}_3\text{CO}_2^-$  in water and heavy water was obtained at 1413.5  $\text{cm}^{-1}$  and 1418.6  $\text{cm}^{-1}$  respectively and for  $\text{CD}_3\text{CO}_2^-$  in water and heavy water, the symmetric stretch was obtained at 1407.5  $\text{cm}^{-1}$  and 1412.4  $\text{cm}^{-1}$ , respectively. Coupling of the intramolecular acetate bands is fairly extensive and therefore DFT calculations were carried out on discrete acetate–water (heavy water) clusters. The clusters with the general stoichiometry  $\text{CH}_3\text{CO}_2^-\cdot n\text{H}_2\text{O}\cdot m\text{H}_2\text{O}$  ( $n = 1\text{--}5$ ,  $m = 1$ ) and  $n$  the number of first shell water molecules and  $m$  the second shell were considered and calculations at the B3LYP 6-311++G(3df,2pd) level were performed. The frequency calculations on  $\text{CH}_3\text{CO}_2^-\cdot 5\text{H}_2\text{O}$  and  $\text{CD}_3\text{CO}_2^-\cdot 5\text{H}_2\text{O}$  clusters supported the assignments of the fundamental modes. The geometrical parameters such as bond length and bond angles of acetate in solution state were obtained. The influence of acetate on the O–H stretching band of water was measured as a function of concentration in order to determine the influence of the methyl group on the structure of water. No enhancement of the water structure around the nonpolar methyl group could be detected nor the existence of dangling  $\nu\text{O–H}$  bonds at  $\sim 3670 \text{ cm}^{-1}$ . In  $\text{NaCF}_3\text{CO}_2$  solutions, however, dangling  $\nu\text{O–H}$  bonds could be observed at  $\sim 3670 \text{ cm}^{-1}$  caused by the hydrophobic  $\text{CF}_3$  group. Finally, the nature of the ion pairs formed between  $\text{Na}^+$  and acetate were discussed in  $\text{NaCH}_3\text{CO}_2(\text{aq})$  and in concentrated solutions no contact ion pairs could be detected.

 Received 15th August 2014  
 Accepted 13th February 2015

DOI: 10.1039/c5ra01156f

[www.rsc.org/advances](http://www.rsc.org/advances)

## 1. Introduction

Interest in the study of aqueous carboxylates and carboxylic acids originates from their importance as constituents in biomolecules such as amino acids, fatty acids and surfactants.<sup>1,2</sup> Nuclear magnetic resonance (NMR) experiments revealed a hydration number of 5–6 water molecules for the carboxylate group  $\text{R}-\text{CO}_2^-$  (ref. 3) while X-ray diffraction studies on divalent transition metal acetates gave a hydration number for acetate in

the range between 3.0–6.1.<sup>4</sup> An X-ray study on  $\text{NaCH}_3\text{CO}_2(\text{aq})$ <sup>5</sup> and a neutron diffraction (ND) investigation<sup>6</sup> on  $\text{NaCH}_3\text{CO}_2$  in  $\text{D}_2\text{O}$  reported a hydration number of 4. *Ab initio* molecular orbital calculations indicated relatively strong H-bonds between  $\text{CH}_3\text{CO}_2^-$  oxygen atoms and first shell water molecules.<sup>7,8</sup> Molecular dynamics (MD) simulations demonstrated, furthermore, that the first-shell waters are either loosely or tightly bound to their  $\text{CH}_3\text{CO}_2^-$  oxygen atoms leading to a fluctuation in the hydration number ranging from 2–5.<sup>9</sup> Dielectric relaxation spectroscopic (DRS) measurements on  $\text{NaCH}_3\text{CO}_2(\text{aq})$  aimed at the hydration, dissociation and ion-pair formation were recently reported.<sup>10,11</sup> A combined Raman and infrared spectroscopic investigation on  $\text{NaCH}_3\text{CO}_2(\text{aq})$  was undertaken and for  $\text{NaCH}_3\text{CO}_2$  solutions, it was established that even up to very high concentrations, the acetate forms solvent separated ion pairs with  $\text{Na}^+$  instead of contact ion pairs and in addition

<sup>a</sup>TU Dresden, Medizinische Fakultät Carl Gustav Carus, Institut für Virologie im MTZ, Fiedlerstr. 42, 01307 Dresden, Germany. E-mail: Wolfram.Rudolph@tu-dresden.de

<sup>b</sup>Technische Universität Bergakademie Freiberg, Institut für Theoretische Physik, Leipziger Str. 23, 09596 Freiberg, Germany

† Electronic supplementary information (ESI) available. See DOI: 10.1039/c5ra01156f

vibrational band assignments of  $\text{CH}_3\text{CO}_2^-$  (aq) were supported by comparison with DFT frequencies.<sup>12</sup>

In this study, we have expanded our work on acetate in aqueous solution to investigate acetate-d<sub>3</sub>,  $\text{CD}_3\text{CO}_2^-$  (aq), by including the vibrational deuterium isotope effect of the C–H bands (Teller-Redlich product rule) as one central point of interest. It became clear, however, that the acetate bands of the hydrated ion were also affected by changing the solvent from water to heavy water even though the  $\text{CH}_3\text{CO}_2^-$  ion possesses no exchangeable hydrogen at room temperature in its molecular structure. (The same holds true for  $\text{CD}_3\text{CO}_2^-$  which does not possess exchangeable deuterium.) This deuterium solvent effect observed for the acetate and acetate-d<sub>3</sub> is the second point of interest in this investigation. Furthermore, the influence of the acetate on the broad O–H stretching band of water and the formation of ion-pairs in  $\text{NaCD}_3\text{CO}_2$ (aq) and  $\text{NaCH}_3\text{CO}_2$ (aq) will be dealt with as well. Raman and infrared spectra of  $\text{NaCH}_3\text{CO}_2$  and  $\text{NaCD}_3\text{CO}_2$  were measured in solution of water and heavy water over a very broad concentration range. Raman spectra were measured to low frequencies at  $\sim 40 \text{ cm}^{-1}$ , the terahertz spectral region, which is of current interest studying electrolyte solutions.<sup>13</sup>

Theoretical frequency calculations assisted in assigning the spectrum of the hydrated acetate and acetate-d<sub>3</sub> ions,  $\text{CH}_3\text{CO}_2^-$  (aq) and  $\text{CD}_3\text{CO}_2^-$  (aq) respectively. Geometrical parameters such as bond length and bond angles were obtained by applying DFT calculations. These parameters have been reported first in the gas phase and then with a polarizable continuum (PC) solvation sphere applying a PC model (PCM) in order to simulate the hydration effect.<sup>12</sup> Theoretical simulations on selected discrete hydration complexes of acetate with water have been carried out. The chosen cluster approach takes into account the directional nature of the H-bonds formed in aqueous solution. DFT frequency calculations on clusters of light acetate,  $\text{CH}_3\text{CO}_2^- \cdot 5\text{H}_2\text{O}$  and  $\text{CH}_3\text{CO}_2^- \cdot 5\text{D}_2\text{O}$ , as well as on fully deuterated acetate,  $\text{CD}_3\text{CO}_2^- \cdot 5\text{H}_2\text{O}$  and  $\text{CD}_3\text{CO}_2^- \cdot 5\text{D}_2\text{O}$  were undertaken. This simple cluster stoichiometry with 5 waters/heavy waters supported the assignments of the intramolecular modes. The different nature of H-bonds formed between acetate and water compared to the ones formed in heavy water (D-bond strength) cannot be addressed by the PC model.

## 2. Experimental section

### 2.1. Preparation of the solutions

A  $\text{NaCH}_3\text{CO}_2$  stock solution was prepared from dried anhydrous  $\text{NaCH}_3\text{CO}_2$  (99.5% extra pure; Merck, Darmstadt, Germany) with triply distilled water free of  $\text{CO}_2$  by weight. The stock solution was  $5.022 \text{ mol L}^{-1}$  ( $6.506 \text{ mol kg}^{-1}$ ,  $R_w = 8.51$ ). Further  $\text{NaCH}_3\text{CO}_2$  solutions were prepared:  $3.262 \text{ mol L}^{-1}$  ( $3.822 \text{ mol kg}^{-1}$ ,  $R_w = 14.52$ ),  $2.184 \text{ mol L}^{-1}$  ( $2.425 \text{ mol kg}^{-1}$ ,  $R_w = 22.94$ ),  $1.209$  ( $1.280 \text{ mol kg}^{-1}$ ,  $R_w = 43.53$ ),  $0.810$  ( $0.842 \text{ mol kg}^{-1}$ ,  $R_w = 66.17$ ),  $0.161$  ( $0.162 \text{ mol kg}^{-1}$ ,  $R_w = 341.80$ ), and  $0.0325 \text{ mol L}^{-1}$  ( $0.0328 \text{ mol kg}^{-1}$ ,  $R_w = 1702.71$ ). The solutions of sodium acetate react alkaline and the pH value of a  $0.161 \text{ mol L}^{-1}$  solution at  $23^\circ\text{C} = 8.8$ . The acetate solutions were sealed in plastic, air tight bottles in order to prevent the uptake of  $\text{CO}_2$

from air. The solution densities were determined with a pycnometer of  $5.000 \text{ mL}$  volume at  $23 \pm 0.1^\circ\text{C}$ . From the solution densities and the concentrations in  $\text{mol L}^{-1}$ , the concentrations in  $\text{mol kg}^{-1}$  were calculated and from the latter, the  $R_w$  – values were determined.  $R_w$  – values represent the number of moles of water per one mole of salt.

Three  $\text{NaCH}_3\text{CO}_2$  solutions in heavy water (99.9% D; Merck, Darmstadt, Germany) were prepared from dried anhydrous  $\text{NaCH}_3\text{CO}_2$  and heavy water by weight. The following solutions were prepared:  $3.944$ ,  $0.790$  and  $0.262 \text{ mol L}^{-1}$ .

Sodium acetate-d<sub>3</sub>,  $\text{NaCD}_3\text{CO}_2$ , (Aldrich; 99% D) solutions in water were prepared with a concentration at  $2.936 \text{ mol L}^{-1}$  ( $3.377 \text{ mol kg}^{-1}$ ,  $R_w = 16.44$ )  $1.468 \text{ mol L}^{-1}$  ( $1.572 \text{ mol kg}^{-1}$ ,  $R_w = 35.29$ ) and  $0.294 \text{ mol L}^{-1}$  ( $0.298 \text{ mol kg}^{-1}$ ,  $R_w = 185.92$ ).

A sodium acetate-d<sub>3</sub>,  $\text{NaCD}_3\text{CO}_2$  (Aldrich; 99% D) solution in heavy water was prepared with a concentration of  $2.792 \text{ mol L}^{-1}$  and  $0.972 \text{ mol L}^{-1}$ .

Six aqueous  $\text{NaCF}_3\text{CO}_2$  (Sigma-Aldrich; 99%) solutions were prepared from dried anhydrous  $\text{NaCF}_3\text{CO}_2$  and water by weight. The following solutions were prepared:  $3.554 \text{ mol L}^{-1}$  ( $R_w = 12.24$ ),  $2.865 \text{ mol L}^{-1}$  ( $R_w = 15.94$ ),  $1.424 \text{ mol L}^{-1}$  ( $R_w = 35.73$ ),  $0.850 \text{ mol L}^{-1}$  ( $R_w = 61.98$ ) and  $0.427 \text{ mol L}^{-1}$  ( $R_w = 126.78$ ). A hydrous  $\text{NaCF}_3\text{CO}_2$  melt was also prepared at  $9.35 \text{ mol L}^{-1}$  ( $R_w = 2.48$ ).

### 2.2. Raman spectra

Raman spectra were measured in the macro chamber of a T 64000 Raman spectrometer from Jobin Yvon in a  $90^\circ$  scattering geometry at  $(23 \pm 0.1)^\circ\text{C}$ . The solutions have been measured in high precision quartz cuvettes from Hellma Analytics (Müllheim, Germany) which were sealed with an air tight stopper. The spectra were excited with the  $487.98 \text{ nm}$  line of an  $\text{Ar}^+$  laser at a power level of  $\sim 1100 \text{ mW}$  at the sample. After passing the spectrometer in subtractive mode, with gratings of 1800 grooves per mm, the scattered light was detected with a cooled CCD detector.<sup>14,15</sup>  $I_{VV}$  and  $I_{VH}$  spectra were obtained with fixed polarisation of the laser beam by rotating the polarizer at  $90^\circ$  between the sample and the entrance slit to give the scattering geometries:  $I_{VV} = I(Y[ZZ]X) = 45\alpha'^2 + 4\gamma'^2$  and  $I_{VH} = I(Y[ZY]X) = 3\gamma'^2$ . The isotropic spectrum,  $I_{iso}$ , was then constructed:

$$I_{iso} = I_{VV} - 4/3I_{VH} \quad (1)$$

The depolarization ratio,  $\rho$ , was determined according to:

$$\rho = I_{VH}/I_{VV} = 3\gamma'^2/(45\alpha'^2 + 4\gamma'^2) \quad (2)$$

The polarization analyser was calibrated with  $\text{CCl}_4$  before each measuring cycle and adjusted if necessary (for details see ref. 14).

The wavenumber positions have been checked with Neon lines and the peak positions for bands with smaller band width (full width at half height; fwhh) have been determined with an error of  $\pm 0.5 \text{ cm}^{-1}$  and broader bands fwhh  $\geq 25\text{--}30 \text{ cm}^{-1}$  with a precision of  $\pm 1 \text{ cm}^{-1}$ . In dilute solutions, the signal to noise ratio ( $S/N$ ) was excellent for the spectra at  $>450$ .



Band intensities have been determined by fitting the bands using Gaussian–Lorentzian product functions on baseline corrected spectra. Relative band intensities for  $\text{CH}_3\text{CO}_2^-$ (aq), and  $\text{CH}_3\text{CO}^-$ (D<sub>2</sub>O) as well as for  $\text{CD}_3\text{CO}_2^-$ (aq) and  $\text{CD}_3\text{CO}_2^-$ (D<sub>2</sub>O) were presented so that the strongest mode was set to 100 and the band intensities of the other modes relative to this value. Details of the band fitting procedure of the baseline corrected Raman-bands were described elsewhere.<sup>16</sup>

Spectra in *R*-format (Bose–Einstein correction) were obtained. The isotropic spectrum,  $R_{\text{iso}}$  was then constructed similar to eqn (2):  $R_{\text{iso}} = R_{\text{VV}} - 4/3R_{\text{VH}}$ . The isotropic *R*-spectra have been used to characterize the restricted translation band of water and restricted translation band of water and acetate (O–H $\cdots$ O $^*$ ). A more detailed description of the Raman measurements and the construction of the spectra in *R*-format is given in ref. 14 and 17.

### 2.3. Density functional theory calculations

For the purpose of modeling the vibrational frequencies the DFT calculations were performed employing the B3LYP functional with a triple- $\zeta$  basis set 6-311++G(3df,2pd) from the Gaussian 03 program suite.<sup>18</sup> The geometry of the acetate ion was then optimized and frequency calculations allowed the assignments of the fundamental modes. Proper description of anions with electrons which are located, on average, relatively far from the nuclei, require diffuse orbitals and polarization basis sets. The optimization procedure led to the result that the geometry of the  $\text{CH}_3\text{CO}_2^-$  with the dihedral angle  $\varphi = 0^\circ$  is stable and possesses no imaginary frequency. DFT frequency calculations were performed for this stable configuration in the gas phase and in addition in the presence of the solvent (water) by placing the solute within the solvent.<sup>19</sup> The latter was modelled as an isotropic and homogeneous continuum characterized by its dielectric properties. The frequencies were calculated with a floating cavity (a set of interlocking spheres attached to the solute atoms). The electrostatic solute–solution interaction was calculated introducing an apparent charge distribution spread on the cavity surface. The PC model implemented in the GAUSSIAN package was used as described in ref. 19.

A second approach, the discrete cluster approach, was applied in order to model the solvent effects of H<sub>2</sub>O and D<sub>2</sub>O taking into account the directionality of the hydrogen bonds between acetate and water and heavy water. The different strength of H-bonds formed between acetate and water was compared to the ones formed in heavy water, the deuterium bond strength. Acetate–water clusters, with an increasing number of water molecules from 1 to 6 water molecules were optimized with the cluster stoichiometry  $\text{CH}_3\text{CO}_2^- \cdot n\text{H}_2\text{O} \cdot m\text{D}_2\text{O}$  ( $n = 1\text{--}5$ ,  $m = 1$ ) with  $n$  the number of first shell water molecules and  $m$  the second shell water. The H-bonding of the water molecules occurs around the oxygen atoms of the –CO<sub>2</sub> group (the CH<sub>3</sub> group is effected much weaker through hydrophobic interaction). No symmetry constraints were employed for the cluster calculations. The calculated structures were minima on the potential energy surface (PES) confirmed by frequency

calculations to ensure that the structures were local minima. Once a local minimum was found, the structure was perturbed and re-optimized to see if a lower energy local minimum could be found. The second derivative of the energy with respect to the nuclear positions then allows the calculation of the frequencies.

## 3. Results and discussion

From here on the paper is organized as follows: first, the structures and symmetries of acetate–water clusters are presented with particular focus on the cluster with 5 water molecules. Then, a brief discussion of the terahertz frequency region is given, including the spectral influence of the Na<sup>+</sup>(aq) and the restricted translation modes of acetate and water. This is then followed by an examination and assignment of the Raman spectroscopic intramolecular acetate bands in aqueous solutions on  $\text{CH}_3\text{CO}_2^-$  and  $\text{CD}_3\text{CO}_2^-$  using the DFT frequencies of the discrete cluster with 5 water molecules to guide in the assignments. Next, the aqueous solvent isotope effects in light and heavy water for  $\text{CH}_3\text{CO}_2^-$  and  $\text{CD}_3\text{CO}_2^-$  are presented and discussed. A description of the influence of the acetate on the O–H band of water is given including the hydrophobic effect of the methyl group. Finally, the different ion-pairs of acetate with Na<sup>+</sup> formed in these solutions are briefly presented.

### 3.1. Symmetry of the $\text{CH}_3\text{CO}_2^-$ ion and acetate–water clusters

The conformer of the  $\text{CH}_3\text{CO}_2^-$  gas phase ion with the dihedral angle  $\varphi = 0^\circ$  is by 11 cal mol<sup>−1</sup> more stable than the conformer,  $\varphi = 29^\circ$  (ref. 12) (both structures possess  $C_s$  symmetry). The structure of the gas phase ion (bond lengths and angles) for  $\varphi = 0^\circ$  resulted in a non-equivalence of the two oxygen atoms of the –CO<sub>2</sub> group (Fig. 3, ref. 12). Because of the slight energy difference between the two conformers in comparison with the thermal energy quantum  $kT$  (576 cal mol<sup>−1</sup> at 290 K), the calculated frequencies of the two conformers differ nominally from each other and are within the band width of the observed acetate bands.

Applying the PC method to account for the hydration effect in aqueous solution resulted in good frequency values for  $\text{CH}_3\text{CO}_2^-$ (aq)<sup>12</sup> but it is unable to account for the directionality of the H-bonds between acetate and H<sub>2</sub>O. Modeling the influence of solvation (*i.e.* hydration) by applying a structureless PC around the species will not result in calculable frequency changes by going from water to heavy water as a solvent. Water at 25 °C has a  $\epsilon$ -value of 78.54 while D<sub>2</sub>O possesses  $\epsilon = 78.06$ . Such a small difference in  $\epsilon$  cannot explain the change of the acetate frequencies using PCM.

The acetate–water cluster with 5 waters ( $\text{CH}_3\text{CO}_2^- \cdot 5\text{H}_2\text{O}$ ) which will be discussed in greater detail resembles a realistic model for the hydrated acetate ion. The directional nature of the H-bonds for the cluster structure for  $\text{CH}_3\text{CO}_2^- \cdot 5\text{H}_2\text{O}$  is shown in Fig. 1 and the geometrical parameters in Table 1. The  $\text{CH}_3\text{CO}_2^-$  in this cluster possesses a dihedral angle of 14.7° which leads to symmetry  $C_1$ . Including the  $\text{CH}_3\text{CO}_2^- \cdot 5\text{H}_2\text{O}$  cluster, six cluster models of acetate with increasing number of



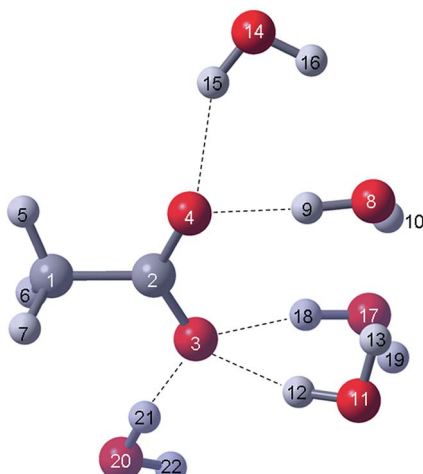


Fig. 1 DFT model of the  $\text{CH}_3\text{CO}_2^- \cdot 5\text{H}_2\text{O}$  cluster. The numbering of the acetate ions (atoms 1–7: C-atoms: 1, 2; O-atoms: 3, 4 and H-atoms 5–7) is the same as for the gas phase cluster given in ref. 12; the oxygen atoms of the five water atoms are labelled 8, 11, 14, 17 and 20. The H-atoms of these water molecules (atoms 9–22) are labelled accordingly.

water molecules (see Experimental section) were optimized and for completeness all results are presented in Table S1† and the structures in Fig. S1.†

From the results of the discrete cluster calculations, it is clear that with an increasing number of water molecules hydrating the oxygen atoms of the  $-\text{CO}_2$  moiety, the following takes place: shortening of the C–C bond distances, change of the dihedral angle  $\neq 0^\circ$  (loss of  $C_s$  symmetry) and the change of the C–O bond lengths of the two C–O bonds leading to a slightly longer bond and one slightly shorter. The acetate water cluster with one water molecule,  $\text{CH}_3\text{CO}_2^- \cdot \text{H}_2\text{O}$  still possesses  $C_s$  symmetry and the water molecule binds in a bifurcated fashion to the two oxygen atoms of the  $-\text{CO}_2$  moiety. The DFT calculations led to a symmetrical geometry and an energy minimum on the PES was obtained (Fig. S1†). However, this is not a realistic model for structural and energetic reasons.<sup>20</sup> Bifurcated bound water molecules with acetate would lead to an artificially narrow restricted translation band at *ca.*  $216\text{ cm}^{-1}$  (DFT result) which is clearly in conflict with the observed broad restricted translation mode of water bound to acetate.<sup>12</sup> For the cluster with  $n = 2$ ,  $\text{CH}_3\text{CO}_2^- \cdot 2\text{H}_2\text{O}$ , the water molecules hydrating the acetate ion form two relatively strong H-bonds with each water molecule yielding slightly different H-bond lengths (Fig. S1 and Table S1†). Due to asymmetric binding of the water molecules, clusters with  $n > 2$  cause the  $\text{CH}_3\text{CO}_2^-$  ion to be distorted ( $\varphi \neq 0^\circ$ ) and its symmetry is, strictly speaking,  $C_1$  ( $C_s$  with small deviations). The cluster with four water molecules reflects a realistic snapshot of the hydration process which was demonstrated by MD calculations.<sup>9</sup> The cluster with six  $\text{H}_2\text{O}$  molecules represents an example of a cluster with 5 waters in the first sphere and the sixth water in the second sphere. From a variety of structural investigations<sup>3–6</sup> and theoretical calculations,<sup>7–9</sup> however, it became evident that the  $-\text{CO}_2$  group is hydrated by  $\sim 5$  water molecules. The geometry optimized  $\text{CH}_3\text{CO}_2^- \cdot 5\text{H}_2\text{O}$

Table 1 Geometrical parameters for the cluster  $\text{CH}_3\text{CO}_2^- \cdot 5\text{H}_2\text{O}$ ; bond lengths  $a_{ij}$  (in Å), angles  $\alpha_{ijk}$  and dihedral angle  $d_{4215}$  of the  $\text{CH}_3\text{CO}_2^-$  ion (see Fig. 1) derived from DFT calculations (B3LYP/6-311++G(3df,2pf))<sup>a</sup>

Parameter	$\text{CH}_3\text{CO}_2^-$ in <i>vacuo</i>	$\text{CH}_3\text{CO}_2^-$ + solvation sphere	$\text{CH}_3\text{CO}_2^- \cdot 5\text{H}_2\text{O}$
$a_{1,2}$	1.561	1.533	1.526
$a_{2,3}$	1.253	1.261	1.269
$a_{2,4}$	1.252 <sub>5</sub>	1.259	1.250
$a_{1,5}$	1.091	1.088	1.087
$a_{1,6}$	1.093	1.091	1.089
$a_{1,7}$	1.093	1.091	1.092
$\alpha_{3,2,4}$	$128.84^\circ$	$125.40^\circ$	$125.03^\circ$
$\alpha_{5,1,6}$	$109.51^\circ$	$109.30^\circ$	$110.55^\circ$
$\alpha_{5,1,7}$	$109.51^\circ$	$109.30^\circ$	$108.88^\circ$
$\alpha_{6,1,7}$	$107.03^\circ$	$107.04^\circ$	$107.18^\circ$
$d_{4,2,1,5}$	$0^\circ$	$0^\circ$	$14.71^\circ$
$a_{3,12}$	n.a.	n.a.	2.032
$a_{3,18}$	n.a.	n.a.	1.947
$a_{3,21}$	n.a.	n.a.	1.780
$a_{4,9}$	n.a.	n.a.	1.756
$a_{4,15}$	n.a.	n.a.	2.016
$a_{3,11}$			2.967
$a_{3,17}$			2.886
$a_{3,20}$			2.762
$a_{4,8}$			2.741
$a_{4,14}$			2.907

<sup>a</sup> n.a. = not applicable.

cluster was used to calculate the second derivative of the energy, with respect to the nuclear positions, in order to yield frequencies of the acetate ion and the water molecules of the first hydration sphere.

The result of the  $\text{CH}_3\text{CO}_2^- \cdot 5\text{H}_2\text{O}$  cluster model describes the hydrated acetate ion in solution quite well (Fig. 1). The numbering of the atoms of the acetate ion is the same as in ref. 12 and thus allows comparison of the parameters with the ones presented in Table 1 (ref. 12). A recent DRS study<sup>10</sup> reported two strong H-bonds with two  $\text{H}_2\text{O}$  molecules with the acetate and a total hydration number of  $\sim 11$  at infinite dilute solution. Five of 11 water molecules weakly and strongly interact with the oxygen atoms of the  $-\text{CO}_2$  unit while the other six water molecules surround the  $\text{CH}_3$  group forming a weakly interacting cluster structure (hydrophobic interaction).<sup>7,10</sup> The PC method does not take into account the directional forces of the H-bonds formed between water and the  $-\text{CO}_2$  moiety of acetate and is not helpful in this context. Although the frequencies derived from the PC model are satisfactory and useful for the assignments of the fundamental modes of  $\text{CH}_3\text{CO}_2^-$ , certain modes deviate quite noticeably from the measured frequencies. The discrete cluster model presented offers a remedy for this problem.

The geometrical parameters of the  $\text{CH}_3\text{CO}_2^- \cdot 5\text{H}_2\text{O}$  cluster model compared with those of the unhydrated acetate ion (Table 1) reveal that the C–C bond distance shortens, the C–O bond distances differ in bond length quite noticeably, and a dihedral angle at  $14.7^\circ$  results in a loss of the symmetry plane and, subsequently, a loss in symmetry ( $C_1$ ).



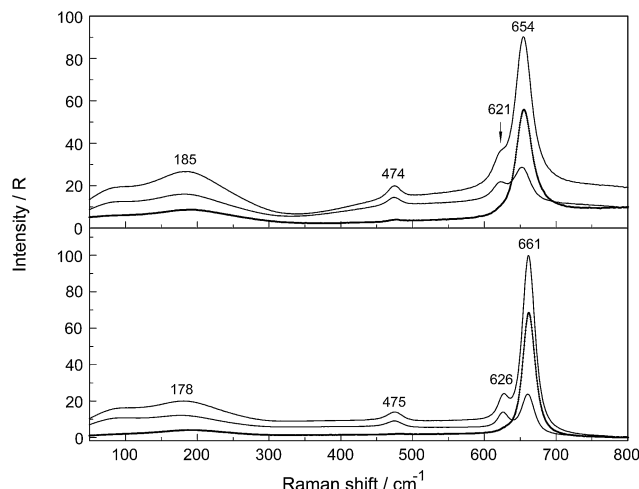


Fig. 2 Comparison of the Raman scattering profiles in *R*-format: polarized, depolarized and isotropic (presented as a thick, dark line) of  $\text{NaCH}_3\text{CO}_2$ (aq). Upper panel:  $2.183 \text{ mol L}^{-1}$  solution in water and lower panel:  $3.944 \text{ mol L}^{-1}$  solution in heavy water. Note, that the deformation mode,  $\delta\text{CO}_2$ , for  $\text{CH}_3\text{CO}_2^-$ (aq) appears at  $654 \text{ cm}^{-1}$  and for  $\text{CH}_3\text{CO}_2^-$ ( $\text{D}_2\text{O}$ ) at  $661 \text{ cm}^{-1}$ .

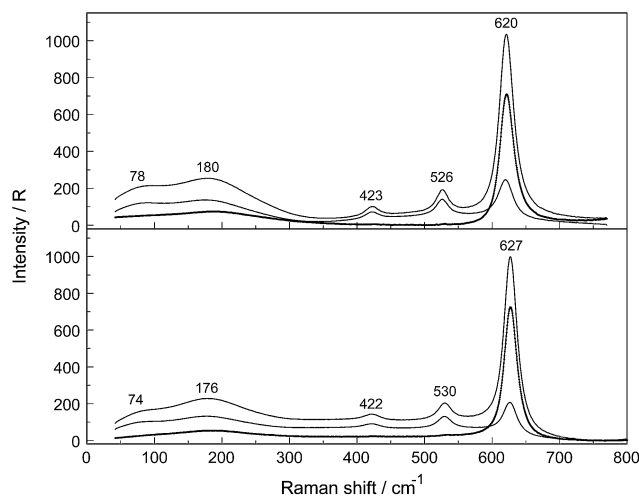


Fig. 3 Comparison of the Raman scattering profiles in *R*-format: polarized, depolarized and isotropic (presented as a thick, dark line) of  $\text{NaCD}_3\text{CO}_2$ (aq). Upper panel:  $2.936 \text{ mol L}^{-1}$  solution in water and lower panel:  $2.792 \text{ mol L}^{-1}$  solution in heavy water. Note, that the deformation mode  $\delta\text{CO}_2$  for  $\text{CH}_3\text{CO}_2^-$ (aq) appears at  $620 \text{ cm}^{-1}$  and for  $\text{CD}_3\text{CO}_2^-$ ( $\text{D}_2\text{O}$ ) at  $627 \text{ cm}^{-1}$ .

### 3.2. The terahertz frequency region of the Na-acetate solutions

Aqueous solutions of  $\text{NaCH}_3\text{CO}_2$  are strongly dissociated in dilute solutions forming  $\text{Na}^+$ (aq) and  $\text{CH}_3\text{CO}_2^-$ (aq) but ion pair formation should be taken into account in concentrated solutions. In  $\text{NaCH}_3\text{CO}_2$  solutions, the ion pairs formed are of the outer-sphere and outer-outer-sphere type with water molecules interposed between  $\text{Na}^+$  and  $\text{CH}_3\text{CO}_2^-$ . The types of ion pairs change significantly with concentration. Completely hydrated  $\text{Na}^+$  and  $\text{CH}_3\text{CO}_2^-$  are formed in very dilute solutions. In more

concentrated solutions, outer-outer-sphere ion-pairs form and in the most concentrated ones ion pairs with one water molecule interposed between  $\text{Na}^+$  and  $\text{CH}_3\text{CO}_2^-$  are formed. The question arises as to whether direct ion pairs are formed in these solutions and this will be discussed in Section 3.4.

A comparison of the Raman spectra in *R*-format in the terahertz frequency region are given in Fig. 2 for  $\text{NaCH}_3\text{CO}_2$  in water and heavy water while the ones for  $\text{NaCD}_3\text{CO}_2$  are given in Fig. 3. The  $\text{Na}^+$  ion in aqueous solution is hydrated and a very broad band at  $\sim 189 \text{ cm}^{-1}$  (isotropic scattering,  $185 \text{ cm}^{-1}$  in the polarized scattering; Fig. 2 upper panel) was detected.<sup>12,21</sup> A neutron scattering study combined with Raman spectroscopic measurements<sup>21</sup> revealed an isotropic band at  $185 \text{ cm}^{-1}$  which is quite close to our value. A  $\text{Na}^+$ -tetra- or -penta-hydrate has to be assumed because our high level DFT cluster calculations revealed that the  $\text{Na}^+$ -hexahydrate is not stable while tetra and penta-aqua  $\text{Na}^+$  clusters are. Both clusters give a quite similar  $\nu_1\text{Na}-\text{O}$  stretching band at  $196$  and  $192 \text{ cm}^{-1}$  respectively. For the deuterated  $\text{Na}^+$ -tetra- and penta-clusters, the peak frequencies were calculated at  $186 \text{ cm}^{-1}$  and  $178 \text{ cm}^{-1}$  respectively in good accord with the measured peak position at  $178 \text{ cm}^{-1}$  in the polarized scattering and at  $180 \text{ cm}^{-1}$  in the isotropic scattering for  $\text{NaCH}_3\text{CO}_2$ ( $\text{D}_2\text{O}$ ) (Fig. 2, lower panel)‡. The calculated frequencies are quite close together and cannot be used to determine which cluster is prevalent. Most of the values for the first hydration number were given at 5 and an internuclear distance  $\text{Na}-\text{O}$  with  $2.34 \text{ \AA}$ .<sup>22,23</sup> Our DFT frequency calculations on  $[\text{Na}(\text{OH}_2)_4]^+$  and  $[\text{Na}(\text{OH}_2)_5]^+$  led to stable structures while  $[\text{Na}(\text{OH}_2)_6]^+$  gave no stable structure. Recent MD modelling confirmed that the  $\text{Na}^+$ -hexa-hydrate is only one of the possible hydrated species along with the tetra- and penta-hydrates.<sup>22-25</sup>

In addition to the  $\text{Na}-\text{O}$  stretching mode at  $189 \text{ cm}^{-1}$  a broad band contribution at  $245 \text{ cm}^{-1}$  appeared (Fig. 2, upper panel) and was assigned to the restricted translation band,  $\nu_s\text{O}-\text{H}\cdots\text{O}$ , reflecting the strong H-bonds between both oxygen atoms of the  $-\text{CO}_2^-$  group and  $\text{H}_2\text{O}$ .<sup>12</sup> This restricted translational mode, determined by acetate water hydrogen bonds, becomes less important with dilution and in dilute acetate solutions this mode appears as a weak polarized band at  $175 \text{ cm}^{-1}$  due to  $\text{O}\cdots\text{H}-\text{O}$  bonds between the water molecules. In  $\text{NaCH}_3\text{CO}_2$  solution in heavy water a similar restricted translation band,  $\nu_s\text{O}-\text{D}\cdots\text{O}$ , reflecting the D-bonds between oxygen atoms of the  $-\text{CO}_2^-$  group and  $\text{D}_2\text{O}$  appears at  $233 \text{ cm}^{-1}$  (see Fig. S2†). A weak polarized band due to  $\text{O}\cdots\text{D}-\text{O}$  bonds between the heavy molecules appears at  $169 \text{ cm}^{-1}$  in neat  $\text{D}_2\text{O}(\text{l})$ .

The cluster with five water molecules (Fig. 1) reveals bond distances of  $\text{O}_{\text{OAc}}\cdots\text{O}_{\text{H}_2\text{O}}$  ( $\text{O}\cdots\text{H}-\text{O}$  nearest-neighbor distances of the H-bond) from  $2.741 \text{ \AA}$  to  $2.967 \text{ \AA}$  (Table 1). These are in good agreement with the experimental values between  $2.77$  and  $2.95$  from X-ray diffraction studies on concentrated divalent transition metal acetates<sup>4</sup> and with a value at  $2.78 \text{ \AA}$  from later measurements on an aqueous  $8 \text{ mol\%}$   $\text{NaCH}_3\text{CO}_2$  solution.<sup>6</sup> Recent neutron scattering data support the X-ray diffraction

‡ For the B3LYP/6-311++G(3df,2pd) level of theory lower DFT frequencies were obtained for the cluster  $[\text{Na}(\text{H}_2\text{O})_6]^+$ . However, this value is insecure because one imaginary frequency was obtained (saddle point).

Table 2 Raman band parameters of  $\text{CH}_3\text{CO}_2^-$  (aq) and  $\text{CH}_3\text{CO}_2^-(\text{D}_2\text{O})$ , assignments and DFT frequencies (data from dilute  $\text{NaCH}_3\text{CO}_2$  in water and heavy water)<sup>a</sup>

$\text{CH}_3\text{CO}_2^-$ (aq)		$\text{CH}_3\text{CO}_2^-(\text{D}_2\text{O})$	
		B3LYP 6-311++(3df,2pd) cluster	
$\nu_{\text{max}}/\text{cm}^{-1}$	fwhh/cm <sup>-1</sup>	Integr. intensity	Depol. ratio
n.d.	—	—	n.d.
474	21	0.254	0.70
620.7	21.3	0.262	0.75
654.2	25.9	2.375	0.346
928.4	11.4	9.874	0.054
1021.5	26.5	0.231	0.70
1052	27	0.032	0.75
1347.6	11	1.884	0.367
1413.5*	24.6	15.07	0.26
1426*	26	0.297	0.5
1440*	18	0.297	0.75
1556	44	1.238	0.62
2935.5	22.5	100.0	0.005
2984	23.5	3.666	0.74
3014	34.6	4.832	0.7
		—	—
		65.9 <sup>+</sup>	474
		483.1	23
		626.8	16
		661.5	20
		926.0 <sup>+</sup>	11.4
		927.2	25.80
		1022	26.5
		1064	1053
		1367	27
		1418.6	11
		1417.8*	22
		1468.3	28
		1429*	1444*
		1485.8	17
		1612.0	42
		3032.9	42
		2936.0	21.5
		2983	24
		3124.7	35
		3016	4.006
		n.d.	—
		—	3124.8
			$\nu_{15}(a'')$
			$\nu_{10}(a')$
			$\nu_{14}(a'')$
			$\nu_9(a')$
			$\nu_8(a')$
			$\nu_{15}(a'')$
			$\nu_{10}(a')$
			$\nu_{14}(a'')$
			$\nu_9(a')$
			$\nu_8(a')$
			$\nu_{15}(a'')$
			$\nu_{10}(a')$
			$\nu_{14}(a'')$
			$\nu_9(a')$
			$\nu_8(a')$
			$\nu_{15}(a'')$
			$\nu_{10}(a')$
			$\nu_{14}(a'')$
			$\nu_9(a')$
			$\nu_8(a')$
			$\nu_{15}(a'')$
			$\nu_{10}(a')$
			$\nu_{14}(a'')$
			$\nu_9(a')$
			$\nu_8(a')$
			$\nu_{15}(a'')$
			$\nu_{10}(a')$
			$\nu_{14}(a'')$
			$\nu_9(a')$
			$\nu_8(a')$
			$\nu_{15}(a'')$
			$\nu_{10}(a')$
			$\nu_{14}(a'')$
			$\nu_9(a')$
			$\nu_8(a')$
			$\nu_{15}(a'')$
			$\nu_{10}(a')$
			$\nu_{14}(a'')$
			$\nu_9(a')$
			$\nu_8(a')$
			$\nu_{15}(a'')$
			$\nu_{10}(a')$
			$\nu_{14}(a'')$
			$\nu_9(a')$
			$\nu_8(a')$
			$\nu_{15}(a'')$
			$\nu_{10}(a')$
			$\nu_{14}(a'')$
			$\nu_9(a')$
			$\nu_8(a')$
			$\nu_{15}(a'')$
			$\nu_{10}(a')$
			$\nu_{14}(a'')$
			$\nu_9(a')$
			$\nu_8(a')$
			$\nu_{15}(a'')$
			$\nu_{10}(a')$
			$\nu_{14}(a'')$
			$\nu_9(a')$
			$\nu_8(a')$
			$\nu_{15}(a'')$
			$\nu_{10}(a')$
			$\nu_{14}(a'')$
			$\nu_9(a')$
			$\nu_8(a')$
			$\nu_{15}(a'')$
			$\nu_{10}(a')$
			$\nu_{14}(a'')$
			$\nu_9(a')$
			$\nu_8(a')$
			$\nu_{15}(a'')$
			$\nu_{10}(a')$
			$\nu_{14}(a'')$
			$\nu_9(a')$
			$\nu_8(a')$
			$\nu_{15}(a'')$
			$\nu_{10}(a')$
			$\nu_{14}(a'')$
			$\nu_9(a')$
			$\nu_8(a')$
			$\nu_{15}(a'')$
			$\nu_{10}(a')$
			$\nu_{14}(a'')$
			$\nu_9(a')$
			$\nu_8(a')$
			$\nu_{15}(a'')$
			$\nu_{10}(a')$
			$\nu_{14}(a'')$
			$\nu_9(a')$
			$\nu_8(a')$
			$\nu_{15}(a'')$
			$\nu_{10}(a')$
			$\nu_{14}(a'')$
			$\nu_9(a')$
			$\nu_8(a')$
			$\nu_{15}(a'')$
			$\nu_{10}(a')$
			$\nu_{14}(a'')$
			$\nu_9(a')$
			$\nu_8(a')$
			$\nu_{15}(a'')$
			$\nu_{10}(a')$
			$\nu_{14}(a'')$
			$\nu_9(a')$
			$\nu_8(a')$
			$\nu_{15}(a'')$
			$\nu_{10}(a')$
			$\nu_{14}(a'')$
			$\nu_9(a')$
			$\nu_8(a')$
			$\nu_{15}(a'')$
			$\nu_{10}(a')$
			$\nu_{14}(a'')$
			$\nu_9(a')$
			$\nu_8(a')$
			$\nu_{15}(a'')$
			$\nu_{10}(a')$
			$\nu_{14}(a'')$
			$\nu_9(a')$
			$\nu_8(a')$
			$\nu_{15}(a'')$
			$\nu_{10}(a')$
			$\nu_{14}(a'')$
			$\nu_9(a')$
			$\nu_8(a')$
			$\nu_{15}(a'')$
			$\nu_{10}(a')$
			$\nu_{14}(a'')$
			$\nu_9(a')$
			$\nu_8(a')$
			$\nu_{15}(a'')$
			$\nu_{10}(a')$
			$\nu_{14}(a'')$
			$\nu_9(a')$
			$\nu_8(a')$
			$\nu_{15}(a'')$
			$\nu_{10}(a')$
			$\nu_{14}(a'')$
			$\nu_9(a')$
			$\nu_8(a')$
			$\nu_{15}(a'')$
			$\nu_{10}(a')$
			$\nu_{14}(a'')$
			$\nu_9(a')$
			$\nu_8(a')$
			$\nu_{15}(a'')$
			$\nu_{10}(a')$
			$\nu_{14}(a'')$
			$\nu_9(a')$
			$\nu_8(a')$
			$\nu_{15}(a'')$
			$\nu_{10}(a')$
			$\nu_{14}(a'')$
			$\nu_9(a')$
			$\nu_8(a')$
			$\nu_{15}(a'')$
			$\nu_{10}(a')$
			$\nu_{14}(a'')$
			$\nu_9(a')$
			$\nu_8(a')$
			$\nu_{15}(a'')$
			$\nu_{10}(a')$
			$\nu_{14}(a'')$
			$\nu_9(a')$
			$\nu_8(a')$
			$\nu_{15}(a'')$
			$\nu_{10}(a')$
			$\nu_{14}(a'')$
			$\nu_9(a')$
			$\nu_8(a')$
			$\nu_{15}(a'')$
			$\nu_{10}(a')$
			$\nu_{14}(a'')$
			$\nu_9(a')$
			$\nu_8(a')$
			$\nu_{15}(a'')$
			$\nu_{10}(a')$
			$\nu_{14}(a'')$
			$\nu_9(a')$
			$\nu_8(a')$
			$\nu_{15}(a'')$
			$\nu_{10}(a')$
			$\nu_{14}(a'')$
			$\nu_9(a')$
			$\nu_8(a')$
			$\nu_{15}(a'')$
			$\nu_{10}(a')$
			$\nu_{14}(a'')$
			$\nu_9(a')$
			$\nu_8(a')$
			$\nu_{15}(a'')$
			$\nu_{10}(a')$
			$\nu_{14}(a'')$
			$\nu_9(a')$
			$\nu_8(a')$
			$\nu_{15}(a'')$
			$\nu_{10}(a')$
			$\nu_{14}(a'')$
			$\nu_9(a')$
			$\nu_8(a')$
			$\nu_{15}(a'')$
			$\nu_{10}(a')$
			$\nu_{14}(a'')$
			$\nu_9(a')$
			$\nu_8(a')$
			$\nu_{15}(a'')$
			$\nu_{10}(a')$
			$\nu_{14}(a'')$
			$\nu_9(a')$
			$\nu_8(a')$
			$\nu_{15}(a'')$
			$\nu_{10}(a')$
			$\nu_{14}(a'')$
			$\nu_9(a')$
			$\nu_8(a')$
			$\nu_{15}(a'')$
			$\nu_{10}(a')$
			$\nu_{14}(a'')$
			$\nu_9(a')$
			$\nu_8(a')$
			$\nu_{15}(a'')$
			$\nu_{10}(a')$
			$\nu_{14}(a'')$
			$\nu_9(a')$
			$\nu_8(a')$
			$\nu_{15}(a'')$
			$\nu_{10}(a')$
			$\nu_{14}(a'')$
			$\nu_9(a')$
			$\nu_8(a')$
			$\nu_{15}(a'')$
			$\nu_{10}(a')$
			$\nu_{14}(a'')$
			$\nu_9(a')$
			$\nu_8(a')$
			$\nu_{15}(a'')$
			$\nu_{10}(a')$
			$\nu_{14}(a'')$
			$\nu_9(a')$
			$\nu_8(a')$
			$\nu_{15}(a'')$
			$\nu_{10}(a')$
			$\nu_{14}(a'')$
			$\nu_9(a')$
			$\nu_8(a')$
			$\nu_{15}(a'')$
			$\nu_{10}(a')$
			$\nu_{14}(a'')$
			$\nu_9(a')$
			$\nu_8(a')$
			$\nu_{15}(a'')$
			$\nu_{10}(a')$
			$\nu_{14}(a'')$
			$\nu_9(a')$
			$\nu_8(a')$
			$\nu_{15}(a'')$
			$\nu_{10}(a')$
			$\nu_{14}(a'')$
			$\nu_9(a')$
			$\nu_8(a')$
			$\nu_{15}(a'')$
			$\nu_{10}(a')$
			$\nu_{14}(a'')$
			$\nu_9(a')$
			$\nu_8(a')$
			$\nu_{15}(a'')$
			$\nu_{10}(a')$
			$\nu_{14}(a'')$
			$\nu_9(a')$
			$\nu_8(a')$
			$\nu_{15}(a'')$
			$\nu_{10}(a')$
			$\nu_{14}(a'')$
			$\nu_9(a')$
			$\nu_8(a')$
			$\nu_{15}(a'')$
			$\nu_{10}(a')$
			$\nu_{14}(a'')$
			$\nu_9(a')$
			$\nu_8(a')$
			$\nu_{15}(a'')$
			$\nu_{10}(a')$
			$\nu_{14}(a'')$
			$\nu_9(a')$
			$\nu_8(a')$
			$\nu_{15}(a'')$
			$\nu_{10}(a')$
			$\nu_{14}(a'')$
			$\nu_9(a')$
			$\nu_8(a')$
			$\nu_{15}(a'')$
			$\nu_{10}(a')$
			$\nu_{14}(a'')$
			$\nu_9(a')$
			$\nu_8(a')$
			$\nu_{15}(a'')$
			$\nu_{10}(a')$
			$\nu_{14}(a'')$
			$\nu_9(a')$
			$\nu_8(a')$
			$\nu_{15}(a'')$
			$\nu_{10}(a')$
			$\nu_{14}(a'')$
</td			

Table 3 Raman band parameters of  $\text{CD}_3\text{CO}_2^-$  (aq) and  $\text{CD}_3\text{CO}_2^-$  ( $\text{D}_2\text{O}$ ), assignments and DFT frequencies (data from dilute  $\text{NaCD}_3\text{CO}_2$  in water and heavy water)<sup>a</sup>

$\text{CD}_3\text{CO}_2^-$ (aq)	$\text{CD}_3\text{CO}_2^-$ ( $\text{D}_2\text{O}$ )				$\text{CD}_3\text{CO}_2^-$ ( $\text{D}_2\text{O}$ )				Numbering of modes and symmetry	Assignment	
	$\nu_{\text{max}}/\text{cm}^{-1}$	fw/hh/cm <sup>-1</sup>	Integr. intensity	Depol. ratio	B3LYP 6-311++ (3df,2pd)	$\nu_{\text{max}}/\text{cm}^{-1}$	fw/hh/cm <sup>-1</sup>	Integr. intensity	Depol. ratio	B3LYP 6-311++ (3df,2pd)	
n.d.	—	—	—	—	39.4 <sup>+</sup>	n.d.	—	—	—	38.8 <sup>+</sup>	$\nu_{15}(a'')$
42.2.5	28.5	1.31	0.71	412.4	421.0	28.5	1.10	0.72	425.2	$\nu_{10}(a')$	$\rho\text{CO}_2$
526.5	19.5	1.48	0.75	531.6 <sup>+</sup>	529.5	24	1.60	0.75	529.3	$\nu_{14}(a'')$	$\rho\text{CO}_2$
621.0	23.5	12.06	0.17	619.8 <sup>+</sup>	627.0	21.5	14.02	0.17	619.0	$\nu_9(a)$	$\delta\text{CO}_2$
834.1	15.0	1.534	0.70	839.3	834.5	10	1.483	0.71	837.8	$\nu_8(a)$	$\rho\text{CD}_3$
885.2	14.1	29.43	0.037	876.6	882.8	11	35.73	0.038	884.0	$\nu_7(a')$	$\nu\text{C-C}$
937	15	0.216	0.73	940.6	936	15	0.245	0.73	939.0	$\nu_{13}(a'')$	$\rho\text{CD}_3$
1035*	21	0.5	0.6	1059.1	1035*	20	0.4	0.50	1059.0	$\nu_6(a')$	$\delta\text{CD}_2$
1043*	38	4.93	0.74	1067.8	1042*	40	5.87	0.754	1067.8	$\nu_{12}(a'')$	$\delta\text{CD}_2$
1086.4	11.4	19.54	0.042	1096.8	1085.8	11.4	20.87	0.042	1096.4	$\nu_5(a')$	$\delta\text{CD}_2$
1407.5	17.5	57.50	0.240	1412.4	1410.5	18.2	62.36	0.240	1414.3	$\nu_4(a')$	$\nu\text{sCO}_2$
1546.5	62	12	0.52	1603.0	1551.5	46	9.585	0.52	1606.4	$\nu_{33}(a')$	$\nu_{\text{asCO}_2}$
2112.5	13.4	100	0.006	2178.4	2112.5	13.4	100.0	0.006	2178.4	$\nu_2(a')$	$\nu_{\text{sCD}_3}$
2188	18.4	63.97	—	2288.1	2188	18.4	51.23	0.74	2288.1	$\nu_{11}(a'')$	$\nu_{\text{asCD}_3}$
2265	62	37.20	—	2318.0	2231	20.5	4.94	—	2318.0	$\nu_1(a')$	$\nu_{\text{asCD}_3}$

<sup>a</sup> n.d.: not detected. \* bands severely overlapped.

undisturbed from the broad deformation band of water at 1641  $\text{cm}^{-1}$  as well as the  $\text{CH}_3$  stretching modes which are overlapped by the very broad O-H stretching profile of water.  $\text{CD}_3\text{CO}_2^-$  spectra in  $\text{H}_2\text{O}$  and in  $\text{D}_2\text{O}$  were measured. The Raman data for  $\text{NaCH}_3\text{CO}_2$  and  $\text{NaCD}_3\text{CO}_2$  solutions in heavy water are also given in Tables 2 and 3, respectively.

Inspection of the spectra in Fig. 4 and 5 and the data in Tables 2 and 3 indicates that there are two distinct vibrational regions for the acetate and acetate-d<sub>3</sub>. Regions from 400–1700  $\text{cm}^{-1}$  and from 2800–3100  $\text{cm}^{-1}$  for  $\text{CH}_3\text{CO}_2^-$  were identified and from 400–1700  $\text{cm}^{-1}$  and from 1900–2400  $\text{cm}^{-1}$  for  $\text{CD}_3\text{CO}_2^-$ .

**Discussion of the fundamental modes for  $\text{CH}_3\text{CO}_2^-$  and  $\text{CD}_3\text{CO}_2^-$  in  $\text{H}_2\text{O}$ .** The normal mode with the lowest frequency at 15.1  $\text{cm}^{-1}$  is a pure torsional motion of the  $\text{CO}_2$  group,  $\nu_{15}(a'')$  and could not be observed experimentally. Three bands were observed in the region from 400–700  $\text{cm}^{-1}$  the origin of which can be reasonably attributed to the rocking and deformational modes of the  $-\text{CO}_2$  group. For  $\text{CH}_3\text{CO}_2^-$  (aq), the slightly polarized mode at 474  $\text{cm}^{-1}$  represents a rocking mode of the  $-\text{CO}_2$  group,  $\nu_{10}(a')$  couples quite severely with an out-of-plane deformation mode of the  $\text{CH}_3$  group (Fig. 2, upper panel). For acetate-d<sub>3</sub>,  $\text{CD}_3\text{CO}_2^-$  (aq), this rocking mode of the  $-\text{CO}_2$  group,  $\nu_{10}(a')$ , appears at lower frequencies namely at 422.5  $\text{cm}^{-1}$  (Fig. 3, upper panel). The Raman mode,  $\nu_{14}(a'')$  at 620.7  $\text{cm}^{-1}$  for  $\text{CH}_3\text{CO}_2^-$  (aq) is depolarized and assigned to an out-of-plane rocking mode of the  $-\text{CO}_2$  group which is strongly coupled with an out-of-plane deformation mode of the  $\text{CH}_3$  group. For  $\text{CH}_3\text{CO}_2^-$  ( $\text{D}_2\text{O}$ ), the mode,  $\nu_{14}(a'')$  is shifted to lower wave-numbers and appears at 526.5  $\text{cm}^{-1}$  (Fig. 3, upper panel). The deformation mode of the  $-\text{CO}_2$  moiety,  $\text{CH}_3\text{CO}_2^-$  (aq),  $\nu_9(a')$ , quite strongly polarized, shows at 654.2  $\text{cm}^{-1}$  and the mode for  $\text{CD}_3\text{CO}_2^-$  (aq) appears at 620.5  $\text{cm}^{-1}$ . The strongest Raman band at 928.4  $\text{cm}^{-1}$  for  $\text{CH}_3\text{CO}_2^-$  (aq) (Fig. 6 upper panel) is assigned to the C-C stretch,  $\nu_8(a')$ , which is strongly polarized but occurs at lower frequencies (885  $\text{cm}^{-1}$ ) in acetate-d<sub>3</sub> (Fig. 7, upper panel). In  $\text{CD}_3\text{CO}_2^-$  (aq) the  $\nu\text{C-C}$  mode is numbered  $\nu_7(a')$ , however, because the rocking mode of the  $\text{CH}_3$  group is shifted due to the deuterium isotope effect to 834.1  $\text{cm}^{-1}$  (Fig. 7, upper panel).§ In the Raman scattering for  $\text{CD}_3\text{CO}_2^-$  (aq), a weakly polarized band of low intensity appears at 834.1  $\text{cm}^{-1}$  and is assigned to a rocking mode of the  $\text{CD}_3$  group numbered  $\nu_8(a')$ . For the undeuterated acetate in aqueous solution, this mode appears at 1021.5  $\text{cm}^{-1}$  as a weak band and is numbered  $\nu_7(a')$ . This large frequency shift is due to the deuterium isotope effect upon substituting D for H. The second librational band of the  $\text{CH}_3$  group of  $\text{CH}_3\text{CO}_2^-$  (aq),  $\nu_{13}(a'')$  occurs at 1052  $\text{cm}^{-1}$ . In the spectrum for acetate-d<sub>3</sub> in aqueous solution,  $\nu_{13}(a'')$  shows at 937  $\text{cm}^{-1}$ . Large vibrational deuterium isotope effects also occur for the bands,  $\nu_6(a')$ ,  $\nu_4(a')$  and  $\nu_{12}(a'')$  for  $\text{CH}_3\text{CO}_2^-$  (aq) at 1347.6  $\text{cm}^{-1}$ , 1426  $\text{cm}^{-1}$  and 1440  $\text{cm}^{-1}$  respectively. The modes at 1347.6  $\text{cm}^{-1}$ , 1426  $\text{cm}^{-1}$ , and 1440  $\text{cm}^{-1}$  are assigned to bending modes of the  $\text{CH}_3$  group (Table 2, Fig. 3 and 6).

§ Note, that the numbering of the bands for  $\text{CD}_3\text{CO}_2^-$  is different from the one for  $\text{CH}_3\text{CO}_2^-$  because of the large isotope shift of the C-D modes (compare fundamental modes in Tables 2 and 3).

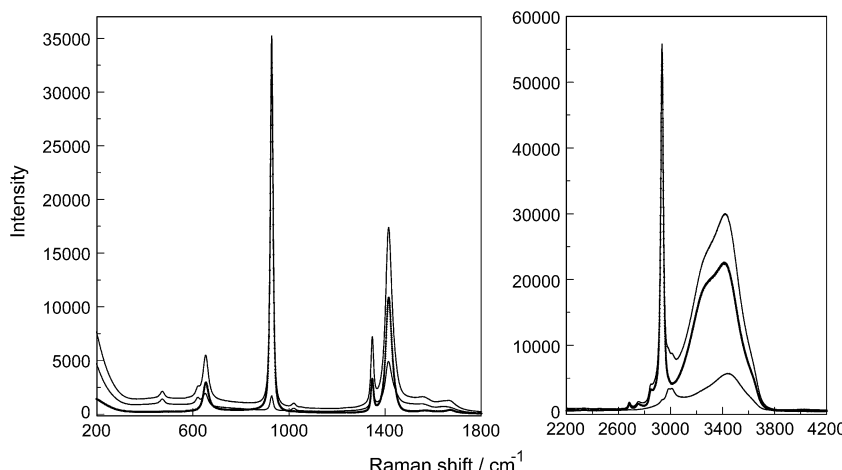


Fig. 4 Overview Raman spectrum of an aqueous solution of  $\text{NaCH}_3\text{CO}_2$  ( $5.022 \text{ mol L}^{-1}$ ). All scattering orientations are given: polarized, depolarized and isotropic which is presented as a thick, dark line. Left panel: Raman bands of  $\text{CH}_3\text{CO}_2^-$ (aq) in the wavenumber range from  $200 - 1800 \text{ cm}^{-1}$ . Right panel contains spectra in the wavenumber range from  $2400 - 4000 \text{ cm}^{-1}$ . Along with the  $\nu\text{C-H}$  modes of  $\text{CH}_3\text{CO}_2^-$ (aq) the very broad O-H stretching band of water is given.

Considering the same bands for acetate- $\text{d}_3$  dissolved in  $\text{H}_2\text{O}$  results in the following band positions: at  $1086.4 \text{ cm}^{-1}$ ,  $1035 \text{ cm}^{-1}$  and  $1043 \text{ cm}^{-1}$  respectively (Table 3). The Raman band at  $1413.2 \text{ cm}^{-1}$  is at  $\rho = 0.26$  quite polarized and assigned to the stretching mode,  $\nu_5(a')$ , of the  $\text{CO}_2$  unit. This mode is strong in the Raman effect and in infrared. However, the symmetric stretch of the  $\text{CO}_2$  group,  $\nu_5(a')$  appears as an asymmetric band due to accidental overlap with the deformation modes of the  $\text{CH}_3$  group (Fig. S2†). The symmetric stretch of the  $-\text{CO}_2$  group for  $\text{CD}_3\text{CO}_2^-$ (aq), now numbered as  $\nu_4(a')$  is strong in Raman and appears as a quite narrow symmetrical band (lift of accidental band overlap) because both deformation modes of the  $\text{CD}_3$  group shifted to much lower frequencies due to the deuterium isotope effect and appear as one broad band at  $\sim 1044 \text{ cm}^{-1}$  (accidental overlap of  $\delta_s$  and  $\delta_{as}$ ; Table 3, Fig. 5 and 7). Two bands at  $1426$  and  $1440 \text{ cm}^{-1}$ , the aforementioned deformation modes of the

$\text{CH}_3$  group, are overlapped almost entirely by the symmetric stretch of the  $-\text{CO}_2$  group and the band appears asymmetric (Fig. 6 and S2†). The Raman band at  $1556 \text{ cm}^{-1}$  is the strongest mode in infrared but fairly weak in Raman and has been assigned to the asymmetric stretch of the  $\text{CO}_2$  group in the spectrum for  $\text{CH}_3\text{CO}_2^-$ (aq), numbered,  $\nu_3(a')$ . In  $\text{CD}_3\text{CO}_2^-$ (aq),  $\nu_3(a')$  occurs as a broad and fairly weak band at  $1547 \text{ cm}^{-1}$ . (For this mode the numbering is the same for the light and the heavy isotopomer.) In the Raman spectra of aqueous solutions, this mode is overlapped by the deformation band of water at  $1641 \text{ cm}^{-1}$  which is broad, quite polarized ( $\rho = 0.14$ ) and shows the non-coincidence effect between the isotropic and anisotropic Raman scattering band positions. For  $\text{CD}_3\text{CO}_2^-$ ( $\text{D}_2\text{O}$ ), the asymmetric stretch of the  $\text{CO}_2$  group occurs at  $1546.5 \text{ cm}^{-1}$  as a weak band free of the overlap from the deformation mode of the water at  $1641 \text{ cm}^{-1}$  (shift of the deformation band of heavy water to  $1206 \text{ cm}^{-1}$ ; Fig. 7).

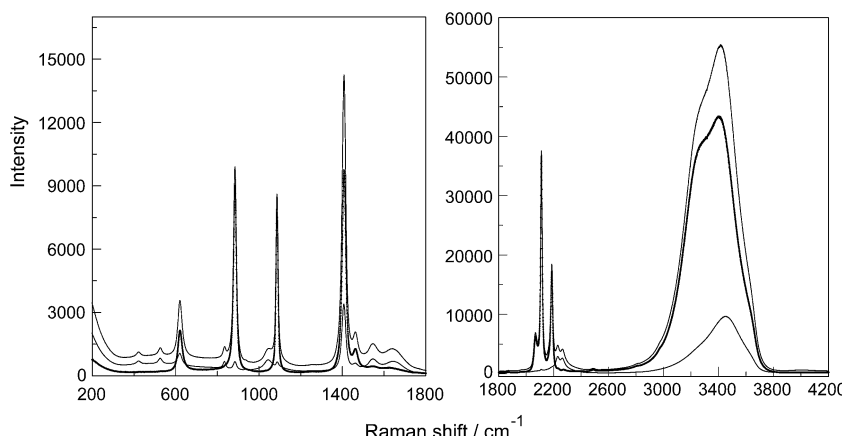


Fig. 5 Overview Raman spectrum of a  $2.936 \text{ mol L}^{-1}$   $\text{NaCD}_3\text{CO}_2$  solution in water. All Raman scattering profiles are given: polarized, depolarized and isotropic which is presented as a thick, dark line). Left panel: Raman bands of the  $\text{CD}_3\text{CO}_2^-$ (aq). Right panel: along with the  $\nu\text{C-D}$  modes of  $\text{CD}_3\text{CO}_2^-$ (aq) the very broad O-H stretching band of water is given.



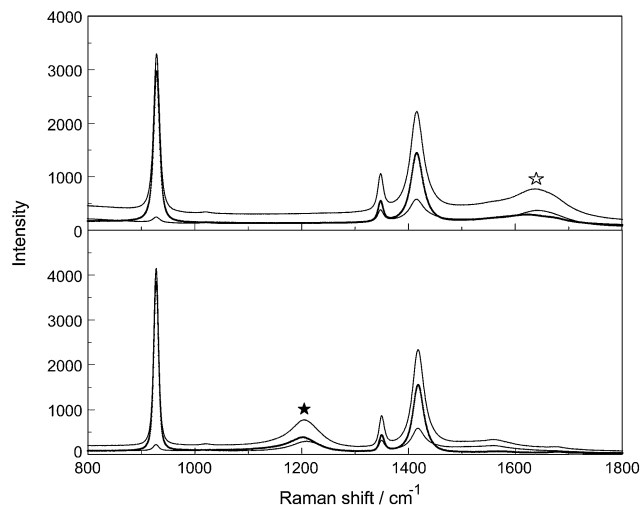


Fig. 6 Comparison of the Raman scattering profiles (polarized, depolarized and isotropic scattering, which is shown as a thick, dark line) of  $\text{NaCH}_3\text{CO}_2$  solutions in water and heavy water. Upper panel:  $1.209 \text{ mol L}^{-1}$  solution in water; lower panel:  $0.790 \text{ mol L}^{-1}$  solution in heavy water. Note, the deformation mode,  $\delta\text{H}_2\text{O}$ , for water at  $1641 \text{ cm}^{-1}$  (upper panel, open star) and at  $1206 \text{ cm}^{-1}$  for  $\text{D}_2\text{O}$ , the deformation mode of heavy water in the lower panel (black star).

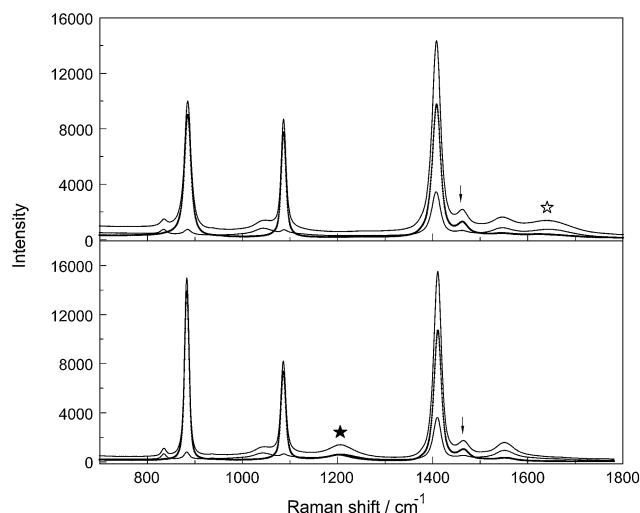


Fig. 7 Comparison of the Raman scattering profiles (polarized, depolarized and isotropic scattering; isotropic scattering shown as a thick, dark line) of  $\text{NaCD}_3\text{CO}_2$  solutions in water and heavy water. Upper panel:  $2.936 \text{ mol L}^{-1}$  solution in water. Lower panel:  $2.792 \text{ mol L}^{-1}$  solution in heavy water. Note the deformation mode  $\delta\text{H}_2\text{O}$  for water at  $1641 \text{ cm}^{-1}$  (upper panel, open star) and at  $1206 \text{ cm}^{-1}$  for  $\delta\text{D}_2\text{O}$  of heavy water in the lower panel (black star). The arrow at  $1463 \text{ cm}^{-1}$  (fwhh =  $24 \text{ cm}^{-1}$ ) indicates the band which is due to an accidental overlap of several combination bands appearing as a relatively strong band ( $\nu_6 + \nu_{10} = 1458 \text{ cm}^{-1}$ ,  $\nu_8 + \nu_9 = 1455 \text{ cm}^{-1}$ ,  $\nu_{13} + \nu_{14} = 1464 \text{ cm}^{-1}$ ; all combinations have  $a'$  symmetry).

The C-H stretching modes are somewhat decoupled from the rest of the vibrational modes and lie above  $2900 \text{ cm}^{-1}$  for the C-H bands and  $2100 \text{ cm}^{-1}$  for the C-D bands (Fig. 2 and 3, left panels). Three bands at  $2935.5 \text{ cm}^{-1}$ , the strongest mode in

Raman,  $\nu_2(a')$  and the much weaker bands at  $2984$  and  $3014 \text{ cm}^{-1}$ , numbered  $\nu_{13}(a'')$  and  $\nu_1(a')$  respectively, are assigned to the stretching bands of the  $\text{CH}_3$  group. The  $\nu_2(a')$ , the  $\nu_s\text{CD}_3$  mode in  $\text{CD}_3\text{CO}_2^-(\text{aq})$  shows a large frequency shift due to the changes in masses from H to D and the corresponding fundamental frequency decreases by the factor  $1/\sqrt{2}$ , the square root of the ratio of masses. The  $\nu_s\text{CD}_3$  mode in  $\text{CD}_3\text{CO}_2^-(\text{aq})$  appears at  $2112.5 \text{ cm}^{-1}$  and the ratio  $\nu_s\text{CD}_3/\nu\text{CH}_3$  has an experimental value of  $0.719$ , compared with the theoretically expected value of  $0.707$ . The discrepancy is attributed to the fact that the C-H/C-D vibrations are not strictly harmonic and may be further complicated by Fermi resonance.<sup>26</sup> One other fact is remarkable, namely, that the peak position of  $\nu_2(a')$  C-H at  $2935.5 \text{ cm}^{-1}$  hardly changes with increasing concentration. However, the fwhh broadens with increasing  $\text{NaCH}_3\text{CO}_2$  concentration by only a few wavenumbers. The fwhh of  $\nu_2(a')$  C-H for a  $5.02 \text{ mol L}^{-1}$   $\text{NaCH}_3\text{CO}_2$  solution is  $23.1 \text{ cm}^{-1}$  and decreases in width with concentration and is  $\sim 21 \text{ cm}^{-1}$  for a solution at zero concentration. (It is noteworthy that a severe broadening and a small wavenumber shift occurs in  $\text{La}(\text{CH}_3\text{CO}_2)_3(\text{aq})^{27}$ ). This fact shows that the C-H bonds are barely influenced by hydration which is believed to be due to the hydrophobic interaction effect. Calculations on  $\text{CH}_4(\text{aq})$  suggests that the methyl group will only contribute *ca.*  $1 \text{ kcal mol}^{-1}$  to  $\Delta H_{\text{hydr}}$  at  $25 \text{ }^\circ\text{C}$  (ref. 8, page 305).

The Teller-Redlich product rule<sup>28,29</sup> proved to be useful for the assignments of the fundamental modes of the isotopomers. This rule was used to check the assignments of the  $\text{CH}_3\text{CO}_2^-$  ion and its deuterated analog,  $\text{CD}_3\text{CO}_2^-$ . For the two species  $a'$  and  $a''$  of the point group  $C_s$  the following formulae apply:

$$\prod_{i=1}^{10} \frac{\nu_{d,i}}{\nu_i} = \left( \frac{m_H}{m_D} \right)^{5/2} \left( \frac{M_d}{M} \right) \left( \frac{I_{d,z}}{I_z} \right)^{1/2} \quad (3a)$$

$$\prod_{i=11}^{15} \frac{\nu_{d,i}}{\nu_i} = \left( \frac{m_H}{m_D} \right)^2 \left( \frac{M_d}{M} \right)^{1/2} \left( \frac{I_{d,x}}{I_x} \right)^{1/2} \left( \frac{I_{d,y}}{I_y} \right)^{1/2} \quad (3b)$$

and for all frequencies the following formula applies:

$$\prod_{i=1}^{15} \frac{\nu_{d,i}}{\nu_i} = \left( \frac{M_d}{M} \right)^{3/2} \left( \frac{I_{d,x}}{I_x} \right)^{1/2} \left( \frac{I_{d,y}}{I_y} \right)^{1/2} \left( \frac{I_{d,z}}{I_z} \right)^{1/2} \left( \prod_{i=1}^7 \frac{m_i}{m_{d,i}} \right)^{3/2} \quad (4)$$

The symbol  $\nu_i(\nu_{d,i})$  denotes the frequencies of the ion (deuterated ion), the index  $I$  numerates the 10 and 5 normal vibrations of the  $a'$  and  $a''$  species, respectively.  $M(M_d)$  are the total masses of the ions,  $I_x, I_y, I_z$  ( $I_{dx}, I_{dy}, I_{dz}$ ) are the moments of inertia about the  $x, y$ , and  $z$  axes through the center of mass,  $m_i(m_{d,i})$  denote the masses of the atoms of the ions. (The  $x, y$  axes were chosen lying in the symmetry plane, the  $z$  axis perpendicular to it.)

The theoretical results for the product of frequency quotients obtained from DFT calculations are:  $\left( \prod_{i=1}^{10} \frac{\nu_{d,i}}{\nu_i} \right)_{\text{th}} = 0.197$ ,  $\left( \prod_{i=11}^{15} \frac{\nu_{d,i}}{\nu_i} \right)_{\text{th}} = 0.247$ , and  $\left( \prod_{i=1}^{15} \frac{\nu_{d,i}}{\nu_i} \right)_{\text{th}} = 0.0487$ .

Inserting the measured Raman frequencies (see Tables 2 and 3), we obtain:

$$\left( \prod_{i=1}^{10} \frac{\nu_{d,i}}{\nu_i} \right)_{\text{exp}} = 0.206, \quad 0.62 \left( \prod_{i=11}^{14} \frac{\nu_{d,i}}{\nu_i} \right)_{\text{exp}} = 0.248, \quad \text{and}$$

$0.62 \left( \prod_{i=1}^{14} \frac{\nu_{d,i}}{\nu_i} \right)_{\text{exp}} = 0.0504$  in reasonable agreement with the theoretical values. Because the torsional vibrations  $\nu_{15}(\nu_{d,15})$  with the lowest frequency values could not be measured, the quotient of the theoretical values was used instead,  $(\nu_{d,15}/\nu_{15})_{\text{exp}} = (\nu_{d,15}/\nu_{15})_{\text{th}} = 0.62$ .

**H<sub>2</sub>O/D<sub>2</sub>O solvent isotope effect on acetate.** Turning to the problem concerning the aqueous solvent isotope effect, the direct comparison of the spectroscopic data of acetate in water and heavy water {CH<sub>3</sub>CO<sub>2</sub><sup>-</sup>(aq) and CH<sub>3</sub>CO<sub>2</sub><sup>-</sup>(D<sub>2</sub>O)} are contrasted in Table 2 and the ones for acetate-d<sub>3</sub> {CD<sub>3</sub>CO<sub>2</sub><sup>-</sup>(aq) and CD<sub>3</sub>CO<sub>2</sub><sup>-</sup>(D<sub>2</sub>O)} in Table 3. Comparative Raman spectra of CH<sub>3</sub>CO<sub>2</sub><sup>-</sup>(aq) and CD<sub>3</sub>CO<sub>2</sub><sup>-</sup>(D<sub>2</sub>O) are presented in Fig. 6 and the ones for the Raman spectra of CD<sub>3</sub>CO<sub>2</sub><sup>-</sup>(aq) and CD<sub>3</sub>CO<sub>2</sub><sup>-</sup>(D<sub>2</sub>O) in Fig. 7. In general, one expects a solvent change from D<sub>2</sub>O to H<sub>2</sub>O should not cause a shift of the acetate fundamental modes or should lead to a slight shift to lower frequencies. Inspection of the vibrational modes of acetate in D<sub>2</sub>O and H<sub>2</sub>O in Table 2 and acetate-d<sub>3</sub> in Table 3 revealed a surprising result, namely, that although in D<sub>2</sub>O some vibrational modes are not shifted at all or shifted only to slightly lower wavenumbers, certain bands shift noticeably to higher wavenumbers compared with the bands measured in light water. In other words, the change from water to heavy water as a solvent markedly influences the vibrational energy levels of dissolved acetate ions.

The frequencies for the CO<sub>2</sub> group increase by changing from H<sub>2</sub>O to D<sub>2</sub>O for both acetate species namely CH<sub>3</sub>CO<sub>2</sub><sup>-</sup> and CD<sub>3</sub>CO<sub>2</sub><sup>-</sup>. For example, for CH<sub>3</sub>CO<sub>2</sub><sup>-</sup>(aq) and CH<sub>3</sub>CO<sub>2</sub><sup>-</sup>(D<sub>2</sub>O) the deformation mode,  $\delta\text{CO}_2$  appears at 654.2 cm<sup>-1</sup> for the former and at 661.5 cm<sup>-1</sup> for the latter, while  $\nu_s\text{CO}_2$  occurs at 1413.5 cm<sup>-1</sup> and at 1418.2 cm<sup>-1</sup>, respectively. The same is true for  $\nu_{as}\text{CO}_2$  which occurs at 1556 cm<sup>-1</sup> in water and at 1563 cm<sup>-1</sup> in heavy water (data in Table 2). For acetate-d<sub>3</sub>, CD<sub>3</sub>CO<sub>2</sub><sup>-</sup>, in water and heavy water,  $\delta\text{CO}_2$  appears at 621 cm<sup>-1</sup> for the former and at 627 cm<sup>-1</sup> for the latter while  $\nu_s\text{CO}_2$  occurs at 1407.5 cm<sup>-1</sup> and at 1410.5 cm<sup>-1</sup>, respectively. The antisymmetric stretch,  $\nu_{as}\text{CO}_2$ , for acetate-d<sub>3</sub> in water and heavy water occurs at 1546 cm<sup>-1</sup> and 1552 cm<sup>-1</sup>, respectively (Table 3). The acetate cluster model with 5 water molecules reflects the H<sub>2</sub>O-D<sub>2</sub>O solvent isotope effect quite well. These DFT frequencies for CH<sub>3</sub>CO<sub>2</sub><sup>-</sup> and CD<sub>3</sub>CO<sub>2</sub><sup>-</sup> in water and heavy water are presented in Tables 2 and 3, respectively. This change of water to heavy water simply means that the deformation mode and the symmetric stretch of the CO<sub>2</sub> group get stiffer in heavy water. This may be due to a simple mass effect but the different hydrogen bond strength *versus* the deuterium bond strength may also play a role. The main reason for this effect comes from the (anharmonic) coupling of the solvent with the solute. Buckingham studied the H-bond strength *versus* D-bond strength by quantum mechanical calculations many years ago and found that in aqueous systems, the D-bond strength is slightly stronger than the H-

bond strength.<sup>30</sup> The aqueous solvent isotope effect for acetate (and other Na-salts of aliphatic carboxylic acids) was first reported from a combination of heats of transfer measured by calorimetry and free energies of transfer obtained from emf measurements.<sup>31</sup> The negative value at  $-34$  cal mol<sup>-1</sup> for the transfer free energy,  $\Delta G_{\text{d} \leftarrow \text{w}}^0$ , going from water to heavy water indicates that this process occurs spontaneously.<sup>31</sup> A great variety of electrolytes and non-electrolytes was reported and summarized in ref. 32 and attempts to explain this phenomenon were put forward applying Gurney's potential.

### 3.4. The influence of acetate on the O-H stretching band of water

The influence of the solute, NaCH<sub>3</sub>CO<sub>2</sub>, on the water spectrum, especially in the O-H stretching region, should allow conclusions about the hydrophobic hydration of the apolar CH<sub>3</sub> group of the acetate with H<sub>2</sub>O. The Raman O-H band profile of NaCH<sub>3</sub>CO<sub>2</sub>(aq) at 5.022 mol L<sup>-1</sup> ( $R_w = 8.5$ ) is displayed in Fig. 4, left panel and the infrared absorption spectrum from 400 to 4000 cm<sup>-1</sup> of an aqueous 2.184 mol L<sup>-1</sup> NaCH<sub>3</sub>CO<sub>2</sub> solution ( $R_w = 22.9$ ) with the one of neat water are presented in Fig. S3.<sup>†</sup> The complete concentration band profiles of three dilute to moderately concentrated aqueous NaCH<sub>3</sub>CO<sub>2</sub> solutions are given in Fig. S4<sup>†</sup> together with the difference spectra of the OH band profiles of the dilute acetate solutions from which the water contributions were subtracted (see Fig. S5<sup>†</sup>). In the neat liquid, the isotropic O-H profile the water O-H band may be fitted with three Gaussian bands, two very broad and strong band contributions at 3211 cm<sup>-1</sup> and 3405.6 cm<sup>-1</sup> (also called the double band) and a shoulder at  $\sim$ 3625 cm<sup>-1</sup> which is also relatively broad (fwhh  $\sim$  125 cm<sup>-1</sup>). The band contribution at 3625 cm<sup>-1</sup> is assigned to the weakly H-bonded H<sub>2</sub>O molecules

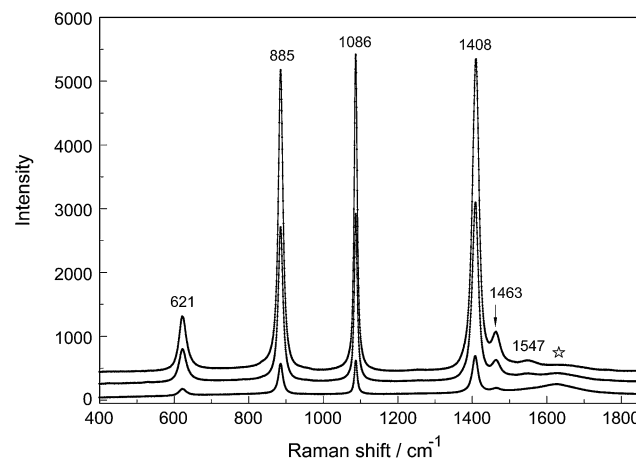


Fig. 8 Concentration profiles of the isotropic scattering of NaCD<sub>3</sub>-CO<sub>2</sub>(aq): from top to bottom: (A) 2.936 mol L<sup>-1</sup>, (B) 1.468 mol L<sup>-1</sup>, 0.294 mol L<sup>-1</sup>. The open star denotes the scattering contribution of the deformation mode of water and the mode denoted by the arrow indicates the combination band at 1463 cm<sup>-1</sup>. The bands at 1408 and 1547 cm<sup>-1</sup> are due to the symmetric stretch of the -CO<sub>2</sub> group while the mode at 885 cm<sup>-1</sup> are the stretching mode of C-C and the mode at 621 cm<sup>-1</sup> is due to the rocking mode of the -CO<sub>2</sub> group. (The strong mode at 1086 cm<sup>-1</sup> is due to the CD<sub>3</sub> deformation mode.)

of the water H-bond network while the band at  $3211\text{ cm}^{-1}$  is assigned to represent the tetrahedrally H-bonded water molecules.<sup>33,34</sup> The isotropic O-H Raman band profile of water of a concentrated  $\text{NaCH}_3\text{CO}_2$  solution was fitted into three Gauss band contributions, as well, positioned at  $3292\text{ cm}^{-1}$ ,  $3455.5\text{ cm}^{-1}$  and a shoulder at  $\sim 3618\text{ cm}^{-1}$  ( $\text{fwhh} = 120\text{ cm}^{-1}$ ). Except for the shift of the two broad and strong band contributions at  $3211$  and  $3406\text{ cm}^{-1}$  for the isotropic O-H band profile, the shoulder at higher wavenumbers is almost unchanged (Fig. 8). A band from dangling H-bonds reported recently at  $3672\text{ cm}^{-1}$  (ref. 35) showing a relatively narrow band width at  $34\text{ cm}^{-1}$  could not be observed for the H-bonds around the methyl group in acetate solutions. The similarity of bulk water at higher wavenumbers in the O-H profile suggests that the water molecules ( $\sim 6$  water<sup>10</sup>) are “clathrate-like” which means three out of four H-bonds are tangential oriented to the  $\text{CH}_3$  surface and one toward the bulk (Fig. 2 of ref. 36). The water structure around the small hydrophobic  $\text{CH}_3$  group is quite similar to the bulk water except for a somewhat slower water-water H-bond exchange kinetic which is only slightly retarded with respect to the bulk water.<sup>36</sup> From theoretical and experimental methods, it turns out that the small  $\text{CH}_3$  group (in contrast to long alkyl chains) does not noticeable change the water structure, its connectivity, nor its H-bond strength.<sup>36,37</sup> In other words, no enhanced hydrophobic hydration can be found around the methyl group of acetate. Furthermore, no signs of dangling O-H bands at  $\sim 3670\text{ cm}^{-1}$  could be observed. However, in contrast to the  $\text{NaCH}_3\text{CO}_2$ (aq) in spectra of aqueous  $\text{NaCF}_3\text{CO}_2$  solutions (see Fig. S6†), measured for comparison, from the dilute to concentrated solution stage a polarized band at  $3671\text{ cm}^{-1}$  ( $\text{fwhh} = 34\text{ cm}^{-1}$ ) clearly indicates “dangling” OH bonds (see our results in Fig. S7†). These dangling OH bonds represent water molecules of the hydrophobic shell surrounding the strongly hydrophobic  $\text{CF}_3$  group and are quite similar to the ones in a water air or a water oil interface.<sup>38,39</sup>

### 3.5. $\text{Na}^+$ -acetate ion pairs

The question of the ion pairs formed in  $\text{Na}^+$  acetate solutions was addressed in our previous publication.<sup>12</sup> However, the solutions of acetate- $d_3$  in aqueous solution and heavy water may be used and studied again to shed light on this question. Raman bands of the  $\text{CO}_2$  group are significant markers for ion pair formation in solution. In conjunction with earlier DRS results, the nature of ion pairs in  $\text{NaCH}_3\text{CO}_2$ (aq) as a function of concentration may be highlighted. DR spectroscopy, a method used to yield information about the character of the ion pairs, reported a sequence of different species: outer-outer-sphere ion pairs, outer-sphere ion pairs but only a small number of contact ion pairs. The latter, if formed in solution should lead to large changes of the acetate bands in  $\text{NaCH}_3\text{CO}_2$ (aq) or a split of the modes into bound or “free” acetate which means non-associated. The formation of contact ion pairs/complexes formed in aqueous solutions was followed but no contact ion pairs could be verified. The advantage of studying the per-deuterated acetate ion,  $\text{NaCD}_3\text{CO}_2$ (aq), is that

the symmetric stretching mode,  $\nu_s\text{CO}_2$ , at  $1407.5\text{ cm}^{-1}$  may be observed undisturbed. In  $\text{NaCH}_3\text{CO}_2$ (aq), however, the symmetric stretch is obscured by the accidental overlap with two  $\text{CH}_3$  deformation modes as discussed above in Section 3.3. The  $\nu\text{C-C}$  mode and also  $\nu_s\text{CO}_2$  impress as narrow and symmetrical bands in  $\text{CD}_3\text{CO}_2^-$ (aq) (Fig. 8) and this indicates that no contact ion pairs of the form  $\text{Na}^+\cdot\text{CH}_3\text{CO}_2^-$  ( $\text{Na}^+\cdot\text{CD}_3\text{CO}_2^-$ ) are formed because bands of the bound acetate will lead to separated bands or visible shoulders separate from the bands of the “free”, hydrated acetate ion. DRS investigations of acetate solutions, however, favored the formation of small amounts of contact ion pairs between  $\text{Na}^+$  and  $\text{CH}_3\text{CO}_2^-$ ,<sup>10</sup> while in a subsequent paper the existence of such ion pairs was denied.<sup>11</sup> Examples of divalent and even trivalent metal ion acetato complexes have been published over the years.<sup>40,41</sup>

## 4. Conclusions

Solutions of the sodium salts of  $\text{CH}_3\text{CO}_2^-$  and  $\text{CD}_3\text{CO}_2^-$  in water and heavy water were studied by Raman and infrared spectroscopy over a broad concentration range and in the wavenumber range from  $40\text{ cm}^{-1}$  to  $4200\text{ cm}^{-1}$ . In the terahertz region the breathing mode of  $[\text{Na}(\text{OH}_2)_n]^+$  ( $n = 4, 5$ ) was characterized at  $189\text{ cm}^{-1}$  and the restricted translation mode of  $\text{CH}_3\text{CO}_2^- \cdots \text{HOH}$  a broad shoulder at  $245\text{ cm}^{-1}$  (see also ref. 12). The acetate/acetate- $d_3$  spectra were assigned according to pseudo  $C_s$  symmetry. Characteristic modes for acetate and acetate- $d_3$  were identified. The two stretching modes of the  $\text{CO}_2$  group,  $\nu_s$  and  $\nu_{as}$ , at  $1413.5\text{ cm}^{-1}$  and  $1556\text{ cm}^{-1}$  respectively at  $1407.5\text{ cm}^{-1}$  and  $1547\text{ cm}^{-1}$  are characteristic. The stretching mode,  $\nu\text{C-C}$  for  $\text{CH}_3\text{CO}_2^-$ (aq), appears at  $928.4\text{ cm}^{-1}$  and the same stretching mode for  $\text{CD}_3\text{CO}_2^-$ (aq) at  $885.2\text{ cm}^{-1}$ . In solutions of heavy water, however, the  $\nu\text{C-C}$  mode appears at  $927.2\text{ cm}^{-1}$  and  $882.8\text{ cm}^{-1}$  respectively. The vibrational isotope effect of the  $-\text{CH}_3$  ( $-\text{CD}_3$ ) group was observed and application of the Teller-Redlich product rule confirmed the frequency assignments.

Coupling of the intramolecular modes are fairly extensive and therefore DFT cluster calculations on  $\text{CH}_3\text{CO}_2^- \cdot 5\text{H(D)}_2\text{O}$  and  $\text{CD}_3\text{CO}_2^- \cdot 5\text{H(D)}_2\text{O}$  were carried out in order to compare the measured spectra with the calculated ones. The geometrical parameters, such as bond length and bond angles of the acetate in solution state, were given.

The possibility of dangling  $\nu\text{O-H}$  bonds was discussed for aqueous  $\text{NaCH}_3\text{CO}_2$  solutions. No evidence for such bonds could be found over the complete concentration range in these solutions in the infrared and Raman spectroscopy. However, in  $\text{NaCF}_3\text{CO}_2$ (aq) dangling  $\nu\text{O-H}$  bands were observed at  $3670\text{ cm}^{-1}$ . A deuterium solvent isotope effect was observed for the intramolecular acetate and acetate- $d_3$  bands in water and heavy water. Finally, the formation process and the nature of the ion pairs formed between  $\text{Na}^+$  and acetate were discussed and it became clear that no contact ion pairs exist even in concentrated  $\text{NaCH}_3\text{CO}_2/\text{NaCD}_3\text{CO}_2$  solutions.



## References

1 B. Hess and N. F. A. van der Vegt, *Proc. Natl. Acad. Sci. U. S. A.*, 2009, **106**, 13296–13300.

2 J. S. Uejio, C. P. Schwartz, A. M. Duffin, W. S. Drisdell, R. C. Cohen and R. J. Saykally, *Proc. Natl. Acad. Sci. U. S. A.*, 2008, **105**, 6809–6812.

3 I. D. Kuntz, *J. Am. Chem. Soc.*, 1971, **93**, 514–516.

4 R. Caminiti, P. Cuccia, M. Monduzzi, G. Saba and G. Crisponi, *J. Chem. Phys.*, 1984, **81**, 543–551.

5 H. Naganuma, Y. Kameda, T. Usuki and O. Uemura, *J. Phys. Soc. Jpn.*, 2001, **70**(suppl. A), 356–358.

6 Y. Kameda, M. Sasaki, M. Yaegashi, K. Tsuji, S. Oomori, S. Hino and T. Usuki, *J. Solution Chem.*, 2004, **33**, 733–745.

7 G. D. Markham, M. Trachtman, C. L. Bock and C. W. Bock, *J. Mol. Struct.*, 1998, **455**, 239–256.

8 G. D. Markham, C. L. Bock and C. W. Bock, *Struct. Chem.*, 1997, **8**, 293–306.

9 A. Payaka, A. Tongraar and B. M. Rode, *J. Phys. Chem. A*, 2010, **114**, 10443–10453.

10 H. M. A. Rahman, G. Heftner and R. Buchner, *J. Phys. Chem. B*, 2012, **116**, 314–323.

11 H. M. A. Rahman and R. Buchner, *J. Mol. Liq.*, 2012, **176**, 93–100.

12 W. W. Rudolph, D. Fischer and G. Irmer, *Dalton Trans.*, 2014, **43**, 3174–3185.

13 I. A. Heisler and S. R. Meech, *Science*, 2010, **327**, 857–860.

14 W. W. Rudolph and G. Irmer, *Appl. Spectrosc.*, 2007, **61**, 1312–1324.

15 W. W. Rudolph, D. Fischer and G. Irmer, *Appl. Spectrosc.*, 2006, **60**, 130–144.

16 W. W. Rudolph, *Z. Phys. Chem.*, 1996, **194**, 73–90.

17 W. W. Rudolph, M. H. Brooker and C. C. Pye, *J. Phys. Chem.*, 1995, **99**, 3793.

18 M. J. Frisch, G. W. Trucks, H. B. Schlegel, G. E. Scuseria, M. A. Robb, J. R. Cheeseman, J. A. Montgomery Jr, T. Vreven, K. N. Kudin, J. C. Burant, J. M. Millam, S. S. Iyengar, J. Tomasi, V. Barone, B. Mennucci, M. Cossi, G. Scalmani, N. Rega, G. A. Petersson, H. Nakatsuji, M. Hada, M. Ehara, K. Toyota, R. Fukuda, J. Hasegawa, M. Ishida, T. Nakajima, Y. Honda, O. Kitao, H. Nakai, M. Klene, X. Li, J. E. Knox, H. P. Hratchian, J. B. Cross, V. Bakken, C. Adamo, J. Jaramillo, R. Gomperts, R. E. Stratmann, O. Yazyev, A. J. Austin, R. Cammi, C. Pomelli, J. W. Ochterski, P. Y. Ayala, K. Morokuma, G. A. Voth, P. Salvador, J. J. Dannenberg, V. G. Zakrzewski, S. Dapprich, A. D. Daniels, M. C. Strain, O. Farkas, D. K. Malick, A. D. Rabuck, K. Raghavachari, J. B. Foresman, J. V. Ortiz, Q. Cui, A. G. Baboul, S. Clifford, J. Cioslowski, B. B. Stefanov, G. Liu, A. Liashenko, P. Piskorz, I. Komaromi, R. L. Martin, D. J. Fox, T. Keith, M. A. Al-Laham, C. Y. Peng, A. Nanayakkara, M. Challacombe, P. M. W. Gill, B. Johnson, W. Chen, M. W. Wong, C. Gonzalez, and J. A. Pople, *Gaussian 03, Revision C.02*, Gaussian, Inc., Wallingford CT, 2004.

19 M. Cossi, G. Scalmani, N. Rega and V. Barone, *J. Chem. Phys.*, 2002, **117**, 43–54.

20 M. Meot-Ner and L. Wayne Sieck, *J. Am. Chem. Soc.*, 1986, **108**, 7525–7529.

21 Y. Kameda, K. Sugarwara, T. Usuki and O. Uemura, *Bull. Chem. Soc. Jpn.*, 1998, **71**, 2769–2776.

22 S. Varma and S. B. Rempe, *Biophys. Chem.*, 2006, **124**, 192–199.

23 R. Mancinelli, A. Botti, F. Bruni, M. A. Ricci and A. K. Soper, *J. Phys. Chem. B*, 2007, **111**, 13570–13577.

24 S. S. Azam, T. S. Hofer, B. R. Randolph and B. M. Rode, *J. Phys. Chem. A*, 2009, **113**, 1827–1834.

25 A. Bankura, V. Carnevale and M. L. Klein, *J. Chem. Phys.*, 2013, **138**, 014501–014510.

26 D. C. McKean, *Spectrochim. Acta, Part A*, 1973, **29**, 1559–1574.

27 W. W. Rudolph and G. Irmer, unpublished results, TU Bergakademie Freiberg 2010.

28 G. Herzberg, *Molecular spectra and molecular structure, II. Infrared and Raman spectra of polyatomic molecules*, Van Nostrand Reinhold Company, New York, 1945, p. 231.

29 O. Redlich, *Z. Phys. Chem., Abt. B*, 1935, **28**, 371–382.

30 A. D. Buckingham and L. Fan-Chen, *Int. Rev. Phys. Chem.*, 1981, **1**, 253–269.

31 H. Snell and J. Greyson, *J. Phys. Chem.*, 1970, **74**, 2148–2152.

32 G. Janeso and W. A. Van Hook, *Chem. Rev.*, 1974, **74**, 689–750, p. 736.

33 B. Auer, R. Kumar, J. R. Schmidt and J. L. Skinner, *Proc. Natl. Acad. Sci. U. S. A.*, 2007, **104**, 14215–14220.

34 B. M. Auer and J. L. Skinner, *J. Chem. Phys.*, 2008, **128**, 224511.

35 P. N. Perera, K. R. Fega, C. Lawrence, E. J. Sundstrom, J. Tomlinson-Phillips and D. Ben-Amotz, *Proc. Natl. Acad. Sci. U. S. A.*, 2009, **106**, 12230–12234.

36 M. Montagna, F. Sterpone and L. Guidoni, *J. Phys. Chem. B*, 2012, **116**, 11695–11700.

37 J. Teixeira and A. Luzar, *Physics of Liquid Water. Structure and Dynamics in Hydration Processes in Biology*, ed. M. C. Bellissent-Funel, IOS Press, Ohmsha, NATO-Science Series, Series A, Life Science-305, 1999, pp. 35–68.

38 N. Ji, V. Ostroverkhov, C. S. Tian and Y. R. Shen, *Phys. Rev. Lett.*, 2008, **100**, 096102.

39 F. G. Moore and G. L. Richmond, *Acc. Chem. Res.*, 2008, **41**, 739–748.

40 G. B. Deacon and R. J. Phillips, *Coord. Chem. Rev.*, 1980, **33**, 227–250.

41 J. E. Tackett, *Appl. Spectrosc.*, 1989, **43**, 483–489.

